

Continuous and Scalable Manufacture of Hybridized Nano-Micro Triboelectric Yarns for Energy Harvesting and Signal Sensing

Liyun Ma,[#] Mengjuan Zhou,[#] Ronghui Wu, Aniruddha Patil, Hao Gong, Shuihong Zhu, Tingting Wang, Yifan Zhang, Shen Shen, Kai Dong, Likun Yang, Jun Wang,* Wenxi Guo,* and Zhong Lin Wang*



Cite This: <https://dx.doi.org/10.1021/acsnano.0c00524>



Read Online

ACCESS |



Metrics & More



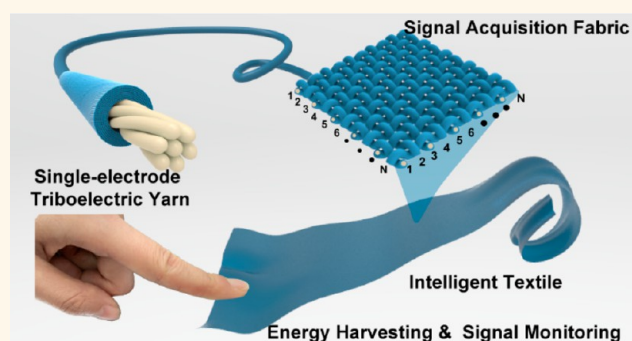
Article Recommendations



Supporting Information

ABSTRACT: Textile-based triboelectric nanogenerators (TENG) that can effectively harvest biomechanical energy and sense multifunctional posture and movement have a wide range of applications in next-generation wearable and portable electronic devices. Hence, bulk production of fine yarns with high triboelectric output through a continuous manufacturing process is an urgent task. Here, an ultralight single-electrode triboelectric yarn (SETY) with helical hybridized nano-micro core-shell fiber bundles is fabricated by a facile and continuous electrospinning technology. The obtained SETY device exhibits ultralightness (0.33 mg cm^{-1}), extra softness, and smaller size ($350.66 \text{ }\mu\text{m}$ in diameter) compared to those fabricated by conventional fabrication techniques. Based on such a textile-based TENG, high energy-harvesting performance (40.8 V , $0.705 \text{ }\mu\text{A cm}^{-2}$, and 9.513 nC cm^{-2}) was achieved by applying a 2.5 Hz mechanical drive of 5 N . Importantly, the triboelectric yarns can identify textile materials according to their different electron affinity energies. In addition, the triboelectric yarns are compatible with traditional textile technology and can be woven into a high-density plain fabric for harvesting biomechanical energy and are also competent for monitoring tiny signals from humans or insects.

KEYWORDS: electrospinning, single-electrode triboelectric yarn, all-yarn-based, biomechanical energy harvesting, biomechanical signal sensing



Garments are textile manufacturing products used by mankind for protection of the human body and as decoration, as well. As an effect of modernization, living standards and lifestyle of people have changed drastically. The traditional functions of clothes (warming and decoration) are no longer sufficient for today's intelligent wearable electronics. More functionalities (*i.e.*, posture and motion monitoring, remote physiological condition tracking, medical rehabilitation training, and portable communication)^{1,2} are pursued by researchers. With regard to major issues such as flexibility, lightness, and comfort, conventional sensors and energy devices are difficult to integrate into textiles due to their bulkiness. Therefore, wearable electronic textiles (E-textiles) have gained significant attention from the research community and textile industry.^{3–5} So far, a great deal of effort has been made to develop E-textiles, such as textile-based sensors, circuits, signal transmission units, calculating components, and energy supply.^{6–8} However, all of these flexible devices need to be recharged frequently and inconveniently or have to be disposed

due to a lack of self-powered capability, resulting in a great waste of resources.

A triboelectric nanogenerator (TENG) can be defined as a self-sufficient power device that converts mechanical movement into electricity in a sustainable and continuous way.⁹ The emergence of TENG textiles is a major breakthrough in the energy field, providing more possibilities for developments in the smart wearable field.^{10,11} However, there are some challenges that must be overcome for the development of energy-harvesting textiles. First, the technology for large-scale production of TENGs is still immature. There are a few scalable

Received: January 19, 2020

Accepted: April 7, 2020

Published: April 7, 2020

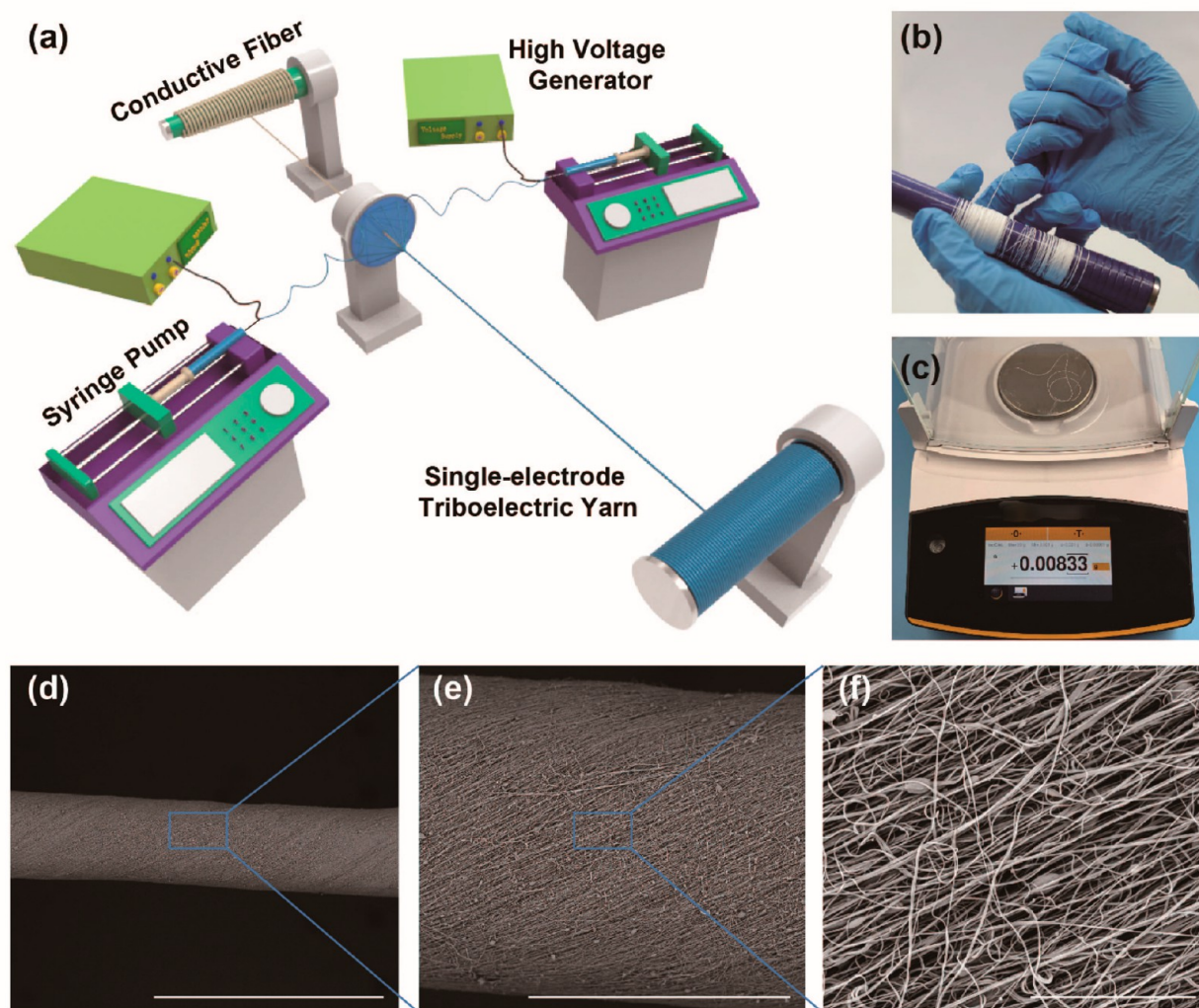


Figure 1. Fabrication process step and images for the nano-micro fiber hybrid SETY. (a) Schematic illustration of SETY fabrication processing. (b) Flexible SETY. (c) Weight of the SETY (whole device) with a length of 25 cm is only 0.00833 g. (d,e) Scanning electron microscopic images for the surface of the SETY in different scales. The scale bars are (d) 1 mm, (e) 300 μm , and (f) 30 μm .

processing methods for TENG textiles,^{12,13} and most of the existing processing methods are restricted by uncontrollable thickness and limited length. Second, the existing fiber-shaped or yarn-shaped TENGs are usually large in diameter, short in length, and uneven in fineness. These “fibers” (“yarns”) are not suitable for fabric processing technology and directly affect weaving efficiency and practicality. Although few studies have attempted to fabricate TENGs from small diameter yarns, the output is too low due to the rigid shell and small contact area.^{14,15} Apart from all of these issues, the softness of the TENG textiles is still a major issue. As we know, the softness of the yarns influences the surface and mechanical properties of the fabric, which has a direct impact on the durability and wearability of the fabric. In addition, the softness of the yarns also affects the style and the visual–tactile properties of the fabric, which directly influences the comfort of the clothing.¹⁶ Although fiber-shaped or yarn-shaped TENGs have been reported previously, little attention is paid to the compatibility with textile technology and comfort properties for human bodies.^{14,17,18}

To address the aforementioned problems, here, ultralight nano-micro fiber hybrid single-electrode triboelectric yarns (SETY) with unlimited length and diameter of $\sim 350 \mu\text{m}$ are

manufactured *via* spinning technology. The SETY, consisting of polyvinylidene fluoride (PVDF) and polyacrylonitrile (PAN) hybrid nanofibers as the shell and conductive silver yarns as the core, has nano-micro helical fiber bundles with a core–shell structure. The instantaneous output electricity can reach 40.8 V, 0.705 $\mu\text{A cm}^{-2}$, and 9.513 nC cm^{-2} upon applying a 2.5 Hz mechanical drive of 5 N. Interestingly, the triboelectric yarns can identify textile materials according to their different electron affinity energies. Moreover, high-density plain fabric is fabricated by weaving the SETYs, which can harvest biomechanical energy and monitor motion signals when touched by human skin (or insects), indicating the potential applications for the triboelectric yarns in wearable electronics.

RESULTS AND DISCUSSION

Continuous Manufacture of the Hybrid Triboelectric Yarns. Here, it is worth noting that the definitions of the yarn and the TENG are different. In the field of textiles, the yarn is defined as a soft elongated subject in which fibers are gathered in the longitudinal direction (*i.e.*, a fiber aggregate).¹⁹ In the TENG, conductive electrodes and electrification materials are

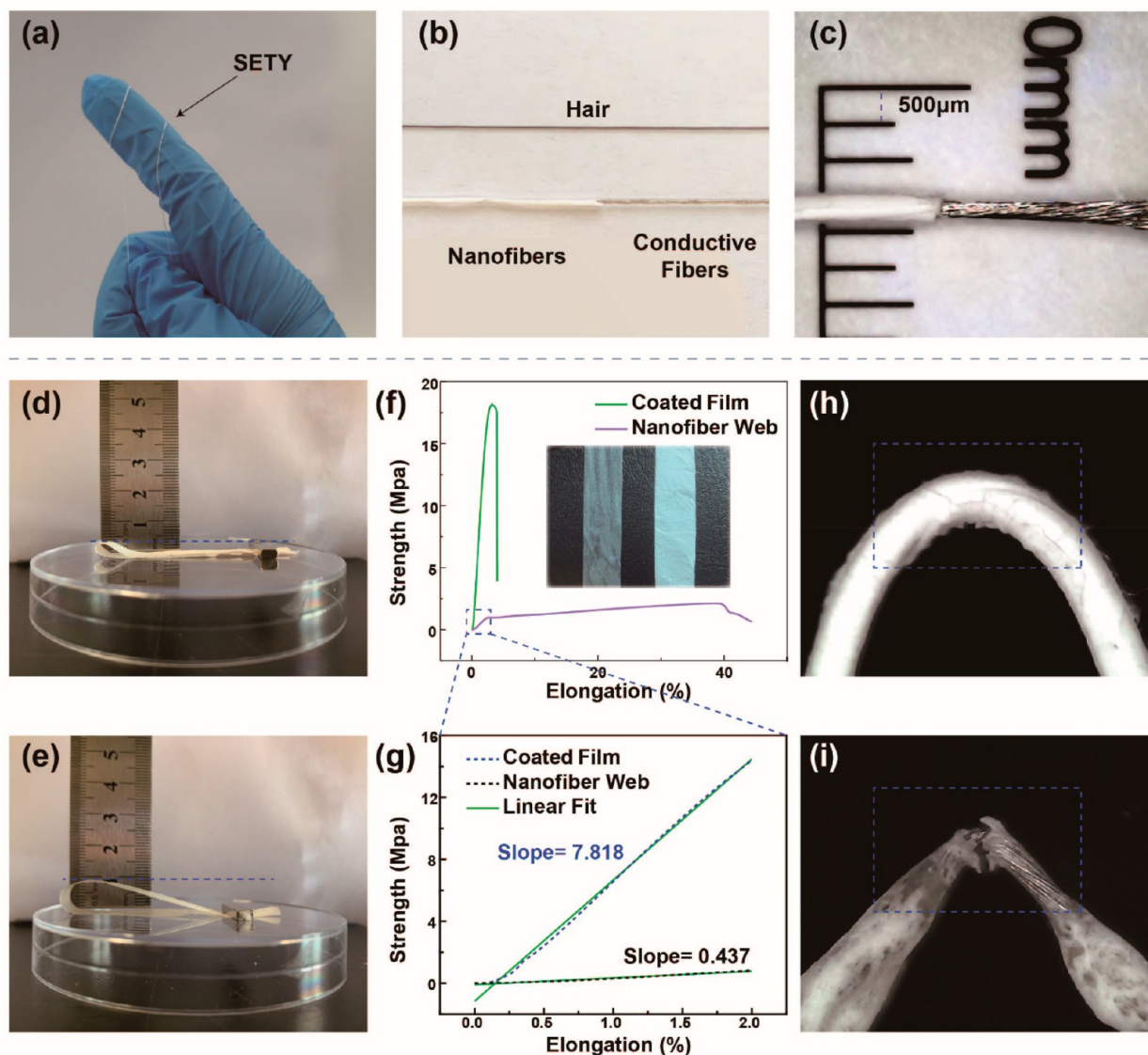


Figure 2. Characterization of fineness and softness of the SETY. (a–c) Visual fineness contrast of the SETY yarn with finger and hair. The flexibility (the distance of the upper and lower ends of the loop) of a nanofiber web (d) and a coated film (e). (f,g) Tensile mechanical properties and Young's modulus of the coated film and nanofiber web. Physical photos of yarn wrapped by the nanofiber web (h) and the coated core-shell yarn with the same material (i) after a plurality of large-angle bending.

two essential materials, which are difficult to integrate into a yarn without jeopardizing their original characteristics, such as softness, thickness, and robustness, in the preparation process. Therefore, a single-electrode type is the most suitable and reasonable for the design of a triboelectric yarn structure.

As shown in Figure 1a, homemade electrospinning equipment with a continuous and automated process is employed to fabricate the SETY. The electrification nanofibers are wrapped around the electrode yarn in one step through the electrospinning setups, which is consistent with textile continuous processing.²⁰ The obtained SETY shows ultralightness, excellent flexibility, and fineness (Figure 1b,c). It is understood that the PVDF and PAN hybrid nanofibers uniformly twine around the conductive yarn with a certain angle (helical fiber bundles), forming a tightly wrapped core-shell structure (Figure 1d–f). The diameter of the whole yarn can be controlled by adjusting the forward speed of the winder.

Fineness and Softness of the SETY. Mechanical flexibility and fineness of textile fibers are two key points to demonstrate the qualities of the fabric, such as deformability, flexibility, and comfort. To achieve this, a coupling technique has been developed that includes traditional textile and electrospinning techniques. As can be seen from Figure 2a, the conductive micro yarn used as the base material of triboelectric yarn is very small in fineness. The diameter of the obtained nano-micro hybrid yarn is $\sim 350 \mu\text{m}$, which can be visually compared with the size of hair, as shown in Figure 2a–c. On the conductive micro yarn support, nanoscale PAN/PVDF hybrid fibers act as electrification materials, wrapped spirally around the conductive yarn to fabricate triboelectric yarn. Thus, the softness of this whole device (core-shell triboelectric yarn) depends on conductive micro yarn and electrification materials. Here, the base material of this triboelectric yarn is conductive yarn with the same flexibility as a normal yarn. In addition, attributed to the continuous electrospinning technique, the obtained PAN/

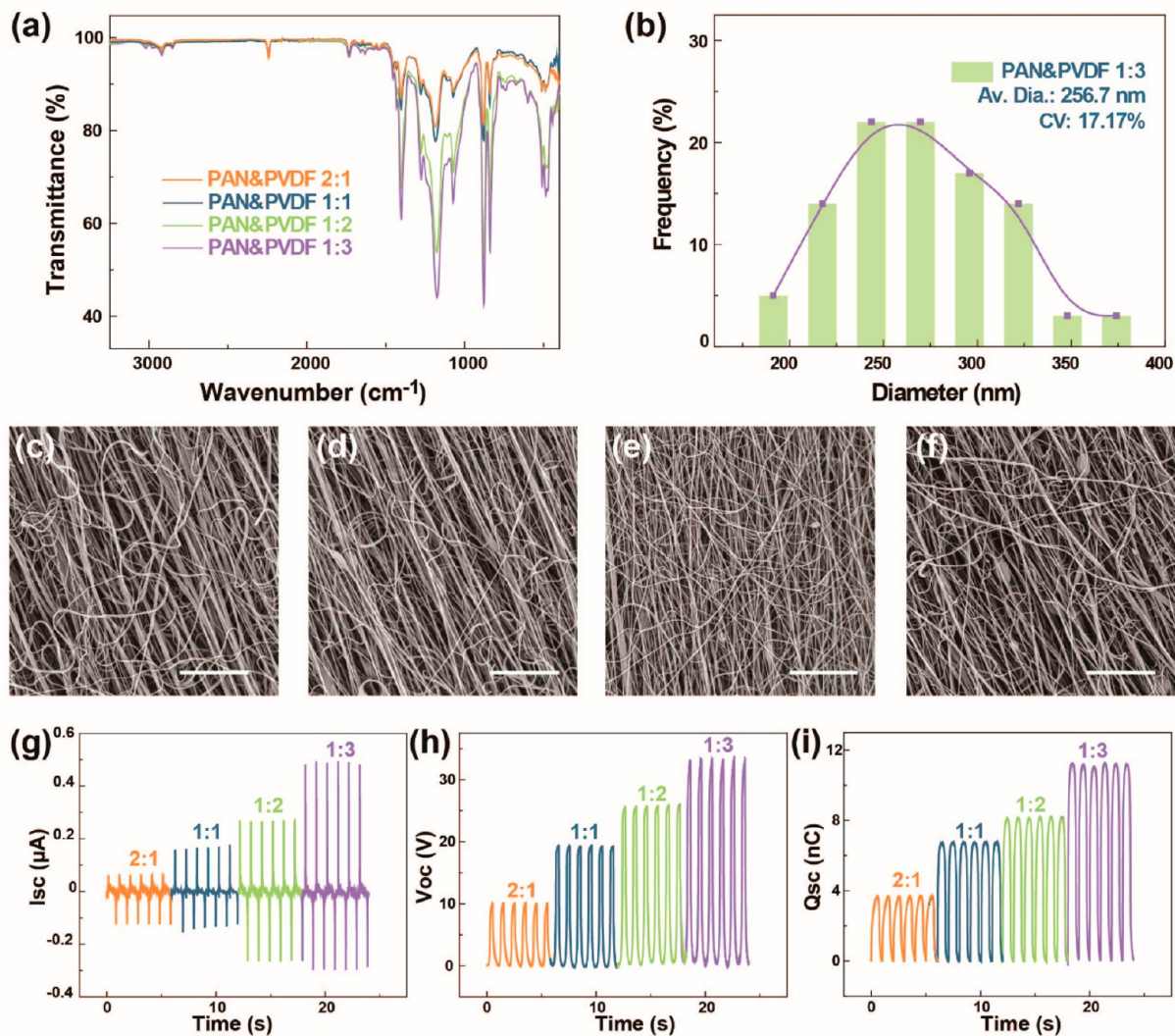


Figure 3. Characterization of electrification materials performance of the SETY. (a) Fourier transform infrared spectra of the electrification materials of the SETY. (b) Average fiber diameters for the PAN/PVDF 1:3 nanofiber webs. (c–f) Magnified scanning electron microscopy images of the (PAN/PVDF 2:1, PAN/PVDF 1:1, PAN/PVDF 1:2, and PAN/PVDF 1:3) nanofiber webs wrapped around the conductive yarn. The scale bars are 15 μm . (g) Short-circuit current, (h) open-circuit voltage, and (i) short-circuit charge quantity of SETY.

PVDF hybrid electrification shell materials tend to be firmly attached around the conductive yarn, which is beneficial for producing very thin and soft SETY.

Compared with the electrification shell materials fabricated by previous coating methods (spin coating, dip coating, layer-by-layer coating, or other methods),¹⁴ the nanofibers obtained by continuous electrospinning technique demonstrate extra softness. The flexibilities of the core–shell triboelectric yarns with nanofibers and the coated film as the shell (the same thickness and material as nanofiber web) are compared by two quantitative tests with the same proportion of materials according to the International Organization for Standardization (ISO) (5979-1982). In the testing, both ends of the nanofiber web and coated film were fixed by a magnet, and as a result, the middle portion of the samples formed flat loops.²¹ The distance of the upper and lower ends of the loop represents the relative flexibility of the film, and the smaller distance implies a better flexibility. The distances of the coated film and nanofibers web are 9 mm and 3.5 mm, respectively, indicating that prepared

nanofiber web exhibits flexibility much better than that of the coated film (Figure 2d,e).

Figure 2f,g further displays the flexibilities of the nanofibers and the coated film by the tensile mechanical properties and Young's modulus. The nanofibers can be stretched to 40%, which is much higher than that of the coated film. Meanwhile, the Young's modulus of the nanofibers is 1 order of magnitude lower than that of the coated film, as displayed in Figure 2g. After a plurality of large-angle bending, the coated core–shell yarn with the same material was broken whereas the yarn wrapped by the nanofibers was intact (Figure 2h,i).

Performance of the Electrification Materials. To investigate the optimized composition of the electrification materials, the PAN and PVDF hybrid nanofibers with different weight ratios of 2:1, 1:1, 1:2, and 1:3 (abbreviated as PAN/PVDF $x:y$) were electrospun. The transmittance characteristic peak of PVDF increases as the amount of PVDF increases in the hybrid yarns (Figure 3a). The diameter distributions of the nanofibers are shown in Figure 3b and Figure S1a,b (Supporting Information), indicating the average diameter for the PAN/

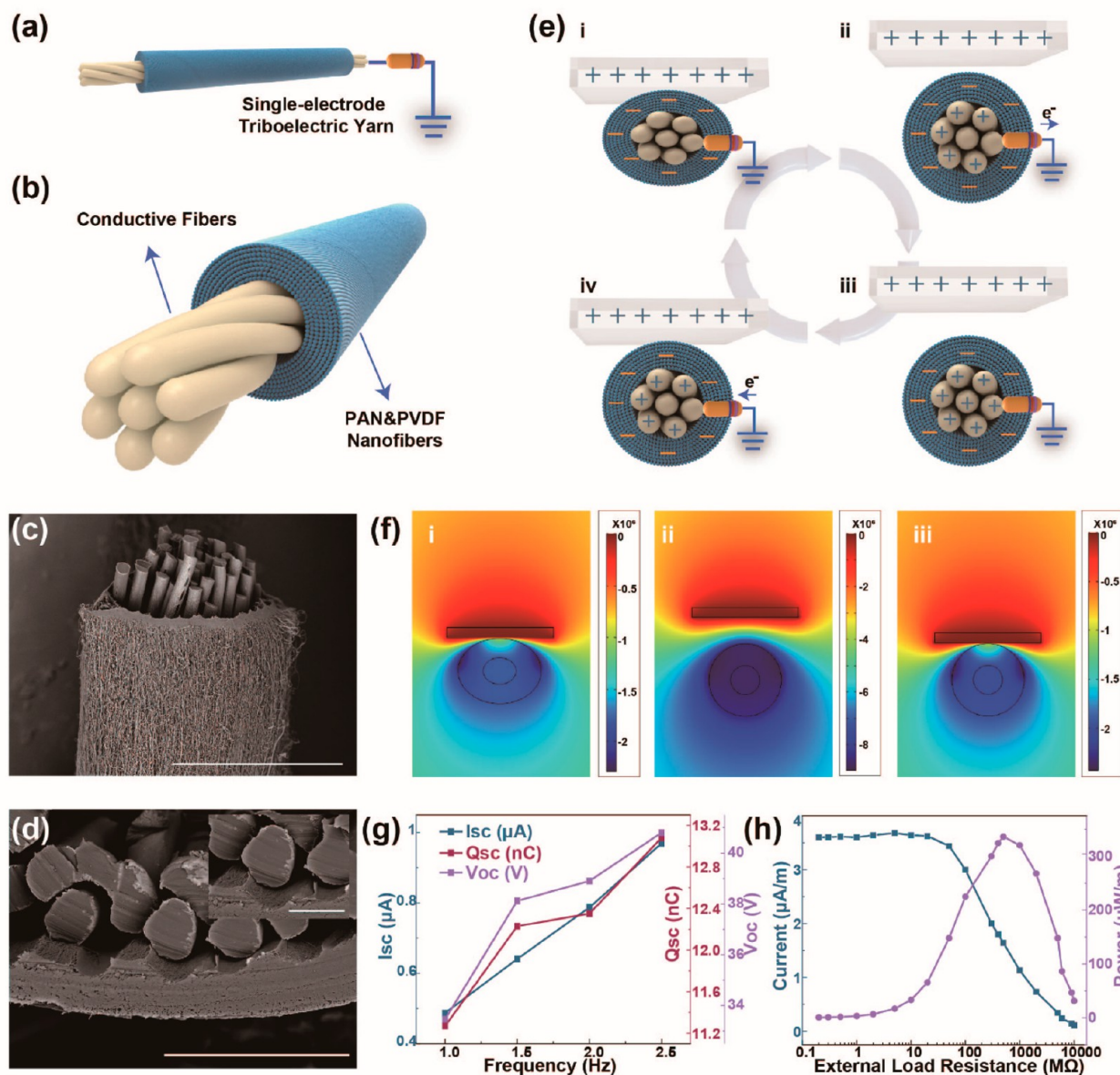


Figure 4. Working principle and basis performances of the SETY. (a,b) Schematic illustration of SETY. (c,d) Scanning electron microscopy images of the cross section of SETY. The scale bars in (c,d) and the illustration inside (d) are 300, 100, and 30 μm , respectively. (f) Numerical calculations of the potential distribution of the SETY at the different states using COMSOL software. (g) Short-circuit current, open-circuit voltage, and short-circuit charge quantity of the SETY measured at different frequencies (1–2.5 Hz). (h) Current and power of the SETY measured at different external load resistances varied from 200 $\text{k}\Omega$ to 10 $\text{G}\Omega$ with a fixed frequency of 1 Hz.

PVDF 1:3 nanofibers is 256.7 nm. In addition, with increasing PVDF content in the precursor solutions, the conductivity and viscosity of the solutions decrease, resulting in an increase in the number of the beads for the spun nanofibers (Figure 3c–f and Figure S1c). The SETYs with different ratios of electrification materials exhibit different output powers. According to the comparison among aforementioned four nanofiber webs, the PAN/PVDF 1:3 sample demonstrated the best performance (Figure 3g–i). It is surprising that such a fine yarn with a length of 25 cm can produce such high electrical properties under low frequency of 1 Hz (the open-circuit voltage (V_{OC}) is up to 33.4 V, short-circuit current (I_{SC}) is 0.49 μA , and the short-circuit charge quantity (Q_{SC}) is 11.2 nC). Attributed to the continuous production process, the yarn can be cut (Figure S2), scaled up, or connected in parallel for energy harvesting, which promotes

its compatibility with textile technology (*i.e.*, weaving, knitting, and braiding). In addition, it can also be used as a thread into any shape for energy collection (Figure S3).

Working Principle of the Single-Electrode Triboelectric Yarns. Figure 4a–d exhibits the schematic illustration and corresponding morphologies of the SETY. The cross-sectional view of the SETY indicates the core yarn is composed of a bundle of micron-sized fibers with diameter of $\sim 25.70 \mu\text{m}$, whereas PAN/PVDF nanofibers are twisted around the yarn, forming a high dense shell with diameter of 24.78 μm .

The working mechanism of the SETY follows the single-electrode mode, whose working principle is schematically shown in Figure 4e. In the SETY, the nanofibers of the shell and the conductive yarn of the core serve as negative triboelectric materials and conductive electrodes, respectively, due to

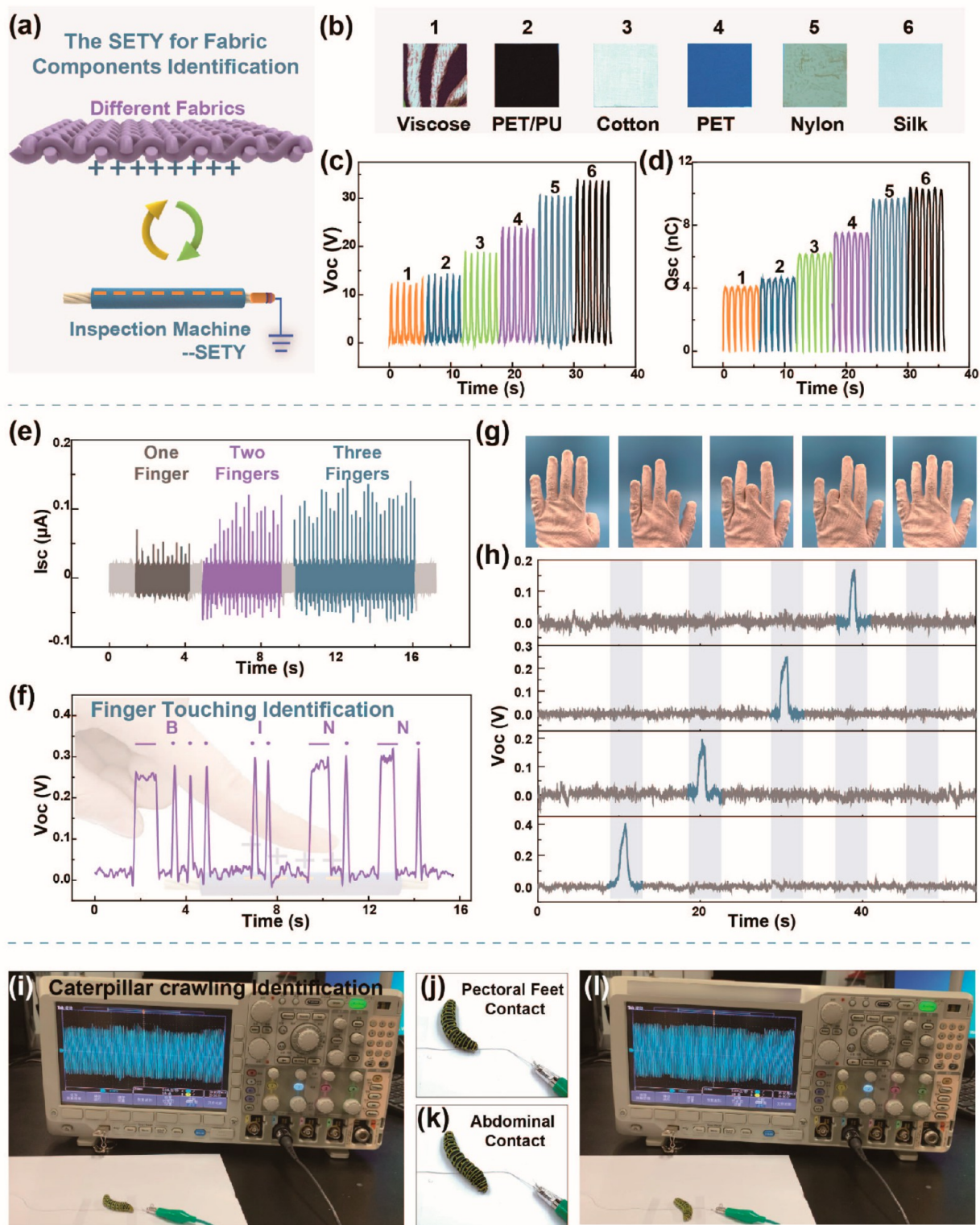


Figure 5. SETY for multifunction inspection and energy collection. (a) Schematic illustration of the SETY for fabric component inspection. (b) Six different fabric samples. (c,d) Open-circuit voltage and short-circuit current inspection signals of six different fabric samples. (e) Different electron signals generated from different finger contact areas *via* changing the number of touching fingertips. (f) Morse code compilation using the intelligent SETY. (g) Photographs of a glove with five pressure sensors implanted on the fingertips. (h) Real-time voltage signals of the five SETY in response to five different finger motions. The caterpillar crawling recognition, *i.e.*, the contact of the feet (i,j) or abdomen (k,l) with the SETY during crawling.

difference in electron affinity potential energies.^{22,23} Based on the triboelectrification and electrostatic induction, the theoretic

cal sources are derived from the Maxwell displacement current, and the mechanism can be described as follows. In the initial

state, due to the lack of external contact with the surrounding, no charge transfer was observed. However, when the skin (or acrylic plate) contacts SETY, charges are transferred from the skin to SETY, which is because of the high surface electron affinity of the PAN/PVDF nanofibers (Figure 4e(i)). As long as relative separation occurs, an electric potential difference will be produced. Technically, the negative charges on the surface of the SETY normally induce positive charges on the conductive yarn, which will compensate the triboelectric charges and allow flow of free electrons from the conductive yarn to the ground (Figure 4e(ii)). When the skin and the SETY are fully separated, the frictional charges are in an equilibrium state, resulting in no electrical power output (Figure 4e(iii)). When the skin touches the SETY again, the induced positive charges on the conductive yarn vanish, causing the opposite flow of the electrons from the ground to the conductive yarn until skin and SETY contact is complete again (Figure 4e(iv)). Thus, the SETY continuously generates an alternating electricity output by the full cycle of the contact and separation process. The electrostatic potential distributions of SETY in the contacting state and separating state are confirmed using numerical simulations *via* COMSOL software, as illustrated in Figure 4f.

Here, the SETY is operated at low frequencies ranging from 1 to 2.5 Hz (Figure 4g and Figure S4), close to that of human movement. As expected, the output performance of the SETY (V_{OC} , I_{SC} , and Q_{SC}) increase with the increase of the driving frequency. Considering the electrical output *versus* the dimensions of the yarn, the electrical performance per unit area of SETY can be calculated as I_{SC}/A and Q_{SC}/A , where A is the effective contact area. As shown in Figure S5, the total external area is 2.75 cm² based on the diameter value of 350.66 μm for the composite yarn. As the yarn is excellent in flexibility, the maximum effective contact area is about 1.375 cm² during the contact process. Thus, the maximum instantaneous output electricity can reach 40.8 V, 0.705 $\mu\text{A cm}^{-2}$, and 9.513 nC cm⁻² upon applying 2.5 Hz driving.

As shown in Figure 4h, the system with contact frequency fixed at 1 Hz follows Ohm's law, in which the output current drops with an increase of the applied external resistances.⁹ The output power achieves a peak value of 336.2 $\mu\text{W m}^{-1}$ instantaneously when the external load resistance is about 500 M Ω . The output power is calculated using equation $W = I^2R$, where I is the output current across the external load and R is the load resistance. The charging ability of SETY is also investigated. With an increase in capacitance (0.1–3.3 μf), a slower charging velocity can be found (Figure S6).

Triboelectric Yarns for Multifunction Sensing and Energy Harvesting. With the development of textile technology, it is urgently needed to develop a technology to quickly identify the ingredients of fabrics. Typically, several steps and methods are required to detect fabric ingredients,^{19,24} such as combustion method, dissolution method, and infrared test, *etc.*, which was found to not only complicate but also damage the original fabric characteristics. Because different fabrics have different electron affinity potential energies,²⁵ it is a simple and convenient method to detect the composition of common fabrics using SETY. As shown in Figure 5a,b, the SETY yarn can be used as a device for the identification and detection of common fabric components. Six common fabrics in contact with the yarn under the same force were examined separately to verify the feasibility of the fabric components. Figure 5c,d shows all the V_{OC} and I_{SC} values of the yarn contacted with viscose fabric, polyester, and polyurethane blend fabric, cotton fabrics,

polyester fabrics, nylon fabric, and silk fabric as the sample fabrics. The generated voltages are 12.6, 14.2, 18.6, 23.7, 30.6, and 33.6 V, respectively. The corresponding charges are 4.0, 4.6, 6.2, 7.5, 9.6, and 10.4 nC, respectively, indicating the SETY is promising to identify the fabric components as per their electron affinity differences.

Two types of contact situations have been observed: one is the textile–textile contact, and another one is the textile and skin contact. In addition to the aforementioned textile and textile contact, the interaction between the textile and human body was found to be more suitable for monitoring human motions that can be applied in human–machine interfacing.²⁶ Based on the higher surface electron affinity of the SETY, it can even detect the electronic signals of fingertip touching and tapping. As shown in Figure 5e and Figure S7, compared with the SETY yarn signal generated by the tapping of the index finger alone, the signal generated by three fingers (the index, middle, and the ring fingers) tapped at the same time is significantly larger, which is because of the enlarged contact area. Also, the intelligent SETY could be applied for Morse code compilation: here, the long-time press specifies the horizontal signal, and the finger tap specifies the dot signal.²⁷ As shown in Figure 5f, when the finger taps the Morse code of a specific character, the corresponding electric signals were recorded in real time that can be used for information delivery after being decrypted by a code translator (*i.e.*, “BINN” or others; Figure S8). In addition, the abilities of harvesting human body energy from touching make the SETY a desirable power source. It is also observed that the SETY can effectively light up 13 light-emitting diodes in series (Movie S1) by manually tapping.

Based on the high sensitivity of the SETY, an intelligent glove for finger gesture identification is designed. It is worth mentioning that the glove is a two-layer design with five independent 10 cm long SETY serpentine stitching the five fingers of the inner glove and the outer glove as the friction layer. The identification of the signal is formed by the friction of the outer layer glove with the inner layer SETY during the bending of the finger. A hand wearing this glove with different gestures is shown in the top of Figure 5g,h, such as keeping all fingers straight or bending different fingers. According to the number of bending fingers, the corresponding hand gestures will be transformed and identified by the output electrical signals. When a finger is bent, a real-time voltage signal is generated. In other words, the instantaneous finger tactile actions can be converted into readable, quantized, and real-time electrical signals through the SETY.

In addition, the SETY can be used to detect caterpillar crawling based on its high sensitivity (Movie S2). It is well-known that the caterpillar has three pairs of pectoral feet near the head and five pairs of abdominal feet on both sides of the abdomen. It is observed that when the caterpillar begins to contact the SETY, noticeable impulse voltage signals appear, indicating an extremely high sensitivity of the SETY (Figure 5i,j). When the head of the caterpillar passes across the SETY, the pectoral feet contact the sensitive yarn, resulting in a short contact signal. While the rest of body is crawling, the abdomen contacts the yarn, generating a long-term contact signal (Figure 5k,l). Therefore, applying the SETY for the detection of caterpillar crawling habits and reproduction has important research value and significance.

Smart Textiles for Biomechanical Sensing. Knittability is an essential parameter for the smart textiles. With the superior flexibility and small thickness, the as-prepared SETY can be

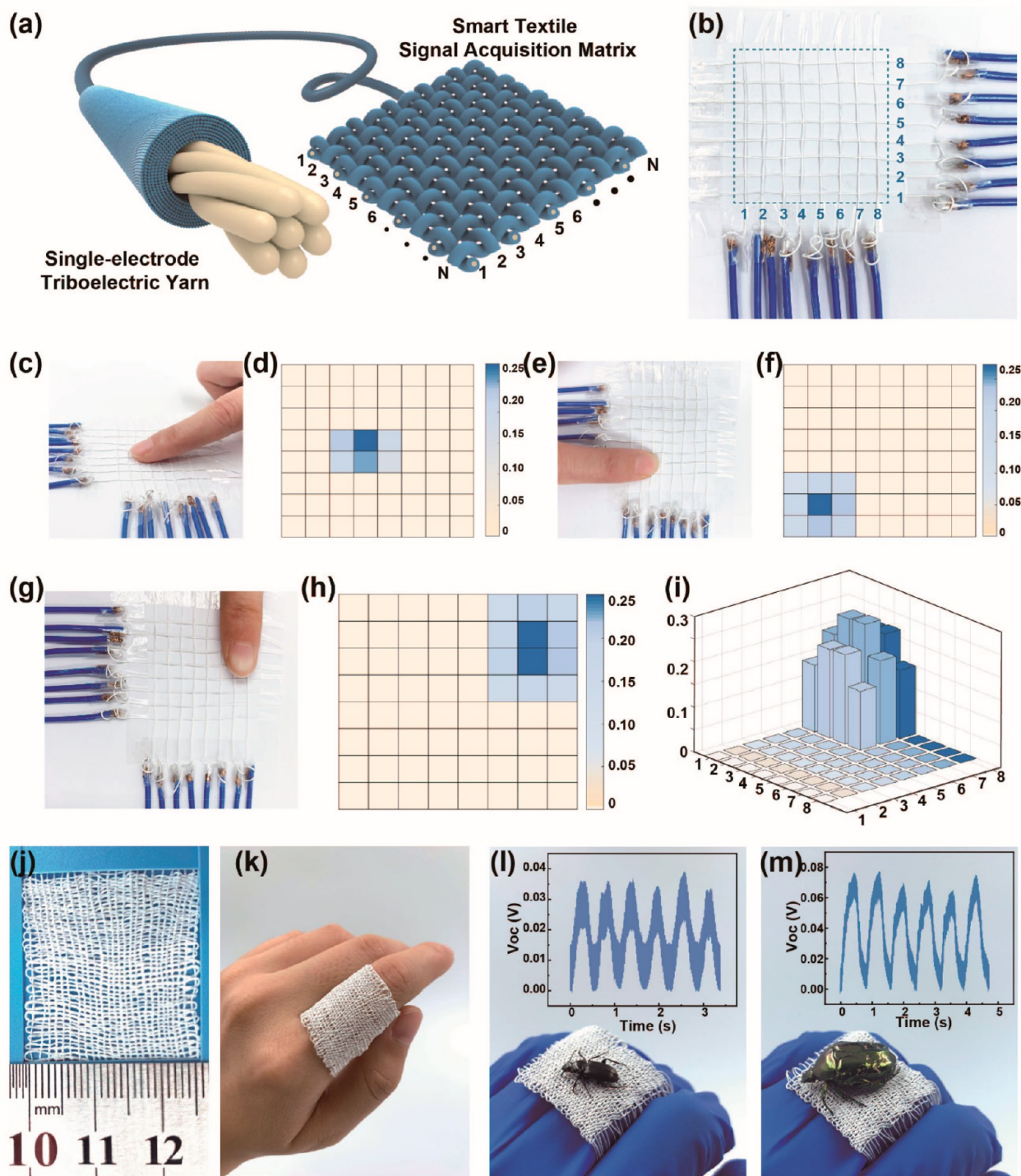


Figure 6. Smart textile for biomechanical sensing. (a,b) Schematic and image of the 8×8 pixel sensing fabric. (c,e,g) Photographs of the 8×8 pixel sensing fabric when a finger was gently pressed on the fabric and the corresponding voltage signals (d,f,h) and the 3D output signals (i). (j,k) Relatively high-density plain fabric fabricated by the SETY. (i,m) Sensitivity measurement of the fabric touched by two different insect specimens.

woven into a smart textile with plain weave structure. To collect quantitative information about the feasibility of tactile sensing for smart textiles, the SETY was fabricated into a textile sensing pattern to spatially map pressure information. The schematic and image of the 8×8 pixel sensing fabric are shown in Figure 6a,b. By putting the finger on the sensing arrays, with the electrical signals of the SETY sensor arrays being monitored by

the arrays, it is able to detect the pressure location and magnitude of the applied load. As shown in Figure 6c–f, an obvious stimulated signal for pressure distribution was generated at the touching area when a finger touched the SETY sensor array.²⁸ At the same time, the pressure exerted on the finger belly is larger than the pressure applied by the fingertip and both sides of the fingers, which is because, when the finger

touched the fabric sensor, a positive pressure is produced, and the contact pressures are distributed differently among the finger belly and other positions. That is to say, the fabric sensor is able to clearly identify the applied pressure position on the sensory matrix. Figure 6g–i reveals information about the optical images, signal output, and pressure distribution (Figure 6i) when a finger generates pressure at the corner of the coplanar SETY sensor. These results clearly demonstrate the capability of the SETY sensing fabric, which shows enough potential, which can be applied to the human–machine interfaces to ultimately detect human activity.

Importantly, the SETY is compatible with traditional textile technology and can be woven into a high-density plain fabric by homemade device (Figure 6j). As can be seen from Figure 6k, the fabric can be wrapped around the fingers, exhibiting good softness and comfort on skin. The sensitivity of the fabric is illustrated by the contact separation of the insect specimens on the fabric in Figure 6l,m. When a small-volume beetle specimen touches the fabric and separates from it, the fabric generates a small voltage signal, whereas when it is touched with a large-volume specimen, it generates a strong voltage signal.

CONCLUSION

In summary, an ultralight nano-micro hybridized core–shell structured yarn with an average diameter of $350.66\ \mu\text{m}$ was fabricated *via* a facile and continuous spinning technology for energy harvesting. The SETY yields high outputs: $40.8\ \text{V}$, $0.705\ \mu\text{A cm}^{-2}$, and $9.513\ \text{nC cm}^{-2}$ upon being applied with $2.5\ \text{Hz}$ mechanical drive. The yarns can be used for the identification of common fabric components. In addition, the yarn is flexible enough to be applied for energy harvesting at human–machine interfaces or for monitoring signals from human motions. The plain fabric woven with the triboelectric yarns could harvest biomechanical energy and monitor tiny signals from humans or insects. Through the different weaving methods of textiles, the yarns can be developed into a multifunctional wearable electronic textile, which exhibits potential applications in mass production of the smart textiles.

METHODS

Material. Polyvinylidene fluoride (PVDF, $M_w = 275,000$), and *N,N*-dimethylformamide (DMF, AR) were purchased from Sinopharm Chemical Reagent Co., Ltd., China. Polyacrylonitrile (PAN, $M_w = 85,000$) was provided by Sigma-Aldrich (Shanghai) Trading Co., Ltd. Conductive silver yarns were bought from Qingdao Zhiyuan Xiangyu Functional Fabric Co., Ltd. China. All chemicals were used without further purification.

Preparation of Precursor Solutions. For preparation of PVDF and PAN precursor solutions, PVDF powders (19 g) and PAN powders (13.64 g) were put into DMF (100 g), separately, and then both stirred mechanically in a water bath at $70\ ^\circ\text{C}$ for 4 h. Then, PVDF and PAN hybrid solutions with different weight ratios of 1:2, 1:1, 2:1, and 3:1 were obtained by mixing the prepared PVDF and PAN precursor solutions described above and were stirred magnetically for 3 h at room temperature.

Fabrication of E-Spin Nano-Micro Fiber Hybrid Yarns. The core–shell nano-micro hybrid yarns were manufactured continuously *via* a homemade electrospun yarn device with the conjugate principle (Figure 1).¹⁷ Conductive silver yarn as the core yarn was passed through the central metal turntable in the device. The prepared precursor solutions were put into the syringes, forming nanofibers *via* electrospinning wrapped around the core yarn. The distance between the needles and the distance between the needle and metal turntable were adjusted to 15 and 10 cm, separately. Furthermore, with applied voltages of $\pm 12\ \text{kV}$ between the two needles, the solution flow rate of

$0.8\ \text{mL h}^{-1}$, the turntable speed of $250\ \text{r min}^{-1}$, and the take-up roll speed of $1\ \text{m min}^{-1}$ were maintained. The yield of the core–shell nano-micro PAN/PVDF hybrid yarns was $60\ \text{m h}^{-1}$. Scaled production was considered, using the continuous fabrication technology. The price of raw materials (Table S1), the estimated costs for SETYs are shown in Table S2. The nano-micro fiber PAN and PVDF hybrid yarns fabricated from different concentration solutions were abbreviated as PAN/PVDF $-x:y$.

Measurement and Characterization. The morphologies of the hybrid yarns and the surface morphologies of fiber webs were analyzed by scanning electron microscopy (TM3000, Hitachi Group, Japan). ImageJ software (NIH, America) was used to calculate the diameter distribution of sub-microfibers, which was calculated by measuring a minimum of 100 fibers. Appearance of the hybrid yarn was characterized by electron microscopy (Dongguan Bigao Electronics Co., Ltd.). The conductivity and viscosity of precursor solutions were examined and recorded using a conductivity meter (Seven2Go, Mettler-Toledo, Switzerland) and rotary viscometer (DV3T, Brookfield Ltd., America), respectively, with Rv-04 rotor and 60 rpm. The coated film was made with a MSK-AFA-ES200 infrared heating tape casting machine (Shenzhen Kejing Zhida Co., Ltd.). The mechanical properties and chemical structures of the webs were tested on a fiber strength elongation tester (XQ-1, Shanghai Lipu Applied Science Institute, China). The membrane was cut into rectangular specimens with dimensions of $5 \times 40\ \text{mm}^2$ and clamped at the cross-head with a gauge length of 20 mm. The cross-head speed was $20\ \text{mm min}^{-1}$. Fourier transform infrared spectra were obtained on a FTIR spectrometer (Bruker Vertex 80 V) in transmission mode. Yarns of different lengths were pasted on the paper to test the TENG's electrical properties (unless otherwise specified, the test length of the SETY is 25 cm, and the tap strength is 5 N). The TENG fabric was woven by a simple homemade device. The voltage, current, and charge quantity of the yarns were recorded with an electrometer (Keithley 6514).

ASSOCIATED CONTENT

Supporting Information

The Supporting Information is available free of charge at <https://pubs.acs.org/doi/10.1021/acsnano.0c00524>.

Basic performances of the PAN&PVDF materials; output performance of the SETY with different length; SETY has good flexibility and can be used as an energy-harvesting thread; output performance of the SETY at different frequencies; effective contact area during the contact process; capacitor charging ability of the SETY; different V_{OC} signals generated from different finger contact areas *via* changing the number of touching fingertips; Morse code compilation using the intelligent SETY; price of the raw material of the SETY; price of four SETY (Figures S1–S7 and Tables S1 and S2) (PDF)

Movie S1: Lighting up 13 light-emitting diodes with SETY with a length of 25 cm (AVI)

Movie S2: Applying the SETY for the detection of caterpillar crawling habits (AVI)

AUTHOR INFORMATION

Corresponding Authors

Jun Wang – Key Laboratory of Textile Science & Technology, Ministry of Education, College of Textiles, Donghua University, Shanghai 201620, China; Email: junwang@dhu.edu.cn

Wenxi Guo – College of Physical Science and Technology, Fujian Provincial Key Laboratory for Soft Functional Materials Research, Xiamen University, Xiamen 361005, China; orcid.org/0000-0002-0791-9023; Email: wxguo@xmu.edu.cn

Zhong Lin Wang – Beijing Institute of Nanoenergy and Nanosystems, Chinese Academy of Science, Beijing 100083, China; School of Materials Science and Engineering, Georgia Institute of Technology, Atlanta, Georgia 30332-0245, United States; orcid.org/0000-0002-5530-0380; Email: zhong.wang@mse.gatech.edu

Authors

Liyun Ma – Beijing Institute of Nanoenergy and Nanosystems, Chinese Academy of Science, Beijing 100083, China; Key Laboratory of Textile Science & Technology, Ministry of Education, College of Textiles, Donghua University, Shanghai 201620, China; College of Physical Science and Technology, Fujian Provincial Key Laboratory for Soft Functional Materials Research, Xiamen University, Xiamen 361005, China

Mengjuan Zhou – Key Laboratory of Textile Science & Technology, Ministry of Education, College of Textiles, Donghua University, Shanghai 201620, China

Ronghui Wu – Key Laboratory of Textile Science & Technology, Ministry of Education, College of Textiles, Donghua University, Shanghai 201620, China; College of Physical Science and Technology, Fujian Provincial Key Laboratory for Soft Functional Materials Research, Xiamen University, Xiamen 361005, China

Aniruddha Patil – College of Physical Science and Technology, Fujian Provincial Key Laboratory for Soft Functional Materials Research, Xiamen University, Xiamen 361005, China

Hao Gong – College of Physical Science and Technology, Fujian Provincial Key Laboratory for Soft Functional Materials Research, Xiamen University, Xiamen 361005, China

Shuihong Zhu – College of Physical Science and Technology, Fujian Provincial Key Laboratory for Soft Functional Materials Research, Xiamen University, Xiamen 361005, China

Tingting Wang – Beijing Institute of Nanoenergy and Nanosystems, Chinese Academy of Science, Beijing 100083, China

Yifan Zhang – Key Laboratory of Textile Science & Technology, Ministry of Education, College of Textiles, Donghua University, Shanghai 201620, China; College of Physical Science and Technology, Fujian Provincial Key Laboratory for Soft Functional Materials Research, Xiamen University, Xiamen 361005, China

Shen Shen – Beijing Institute of Nanoenergy and Nanosystems, Chinese Academy of Science, Beijing 100083, China

Kai Dong – Beijing Institute of Nanoenergy and Nanosystems, Chinese Academy of Science, Beijing 100083, China

Likun Yang – College of Physical Science and Technology, Fujian Provincial Key Laboratory for Soft Functional Materials Research, Xiamen University, Xiamen 361005, China

Complete contact information is available at:
<https://pubs.acs.org/10.1021/acsnano.0c00524>

Author Contributions

*L.M. and M.Z. contributed equally to this work.

Notes

The authors declare no competing financial interest.

ACKNOWLEDGMENTS

We gratefully acknowledge the financial support by the National Key Research and Development Program of China (Grant No. 2016YFA0202704), Fujian Natural Science Foundation (Grant No. 2017J01104), The Fundamental Research Funds for the Central Universities of China (Grant No. 2019061105), The Science and Technology Project of Xinjiang Uygur Autonomous

Region (Grant No. 2017D14002), and The Fundamental Research Funds for the Central Universities and Graduate Student Innovation Fund of Donghua University (Grant No. CUSF-DH-D-2019051).

REFERENCES

- (1) Boutry, C. M.; Beker, L.; Kaizawa, Y.; Vassos, C.; Tran, H.; Hinckley, A. C.; Pfattner, R.; Niu, S. M.; Li, J. H.; Claverie, J.; Wang, Z.; Chang, J.; Fox, P. M.; Bao, Z. N. Biodegradable and Flexible Arterial-Pulse Sensor for the Wireless Monitoring of Blood Flow. *Nat. Biomed. Eng.* **2019**, *3*, 47–57.
- (2) Tian, X.; Lee, P. M.; Tan, Y. J.; Wu, T. L.; Yao, H.; Zhang, M.; Li, Z.; Ng, K. A.; Tee, B. C.; Ho, J. S. Wireless Body Sensor Networks Based on Metamaterial Textiles. *Nat. Electron.* **2019**, *2*, 243–251.
- (3) Heo, J. S.; Eom, J.; Kim, Y. H.; Park, S. K. Recent Progress of Textile-Based Wearable Electronics: A Comprehensive Review of Materials, Devices, and Applications. *Small* **2018**, *14*, 1703034.
- (4) Yang, J.; Liu, Q.; Deng, Z.; Gong, M.; Lei, F.; Zhang, J.; Zhang, X.; Wang, Q.; Liu, Y.; Wu, Z.; Guo, C. F. Ionic liquid-Activated Wearable Electronics. *Mater. Today Phys.* **2019**, *8*, 78–85.
- (5) Weng, W.; Chen, P.; He, S.; Sun, X.; Peng, H. Smart Electronic Textiles. *Angew. Chem., Int. Ed.* **2016**, *55*, 6140–6169.
- (6) Niu, S.; Matsuhisa, N.; Beker, L.; Li, J.; Wang, S.; Wang, J.; Jiang, Y.; Yan, X.; Yun, Y.; Burnett, W.; Poon, A. S. Y.; Tok, J. B.-H.; Chen, X.; Bao, Z. A Wireless Body Area Sensor Network Based on Stretchable Passive Tags. *Nat. Electron.* **2019**, *2*, 361–368.
- (7) Xu, S.; Jayaraman, A.; Rogers, J. A. Skin Sensors Are the Future of Health Care. *Nature* **2019**, *571*, 319–321.
- (8) Shi, Q. F.; He, T. Y. Y.; Lee, C. More than Energy Harvesting—Combining Triboelectric Nanogenerator and Flexible Electronics Technology for Enabling Novel Micro-/Nano-Systems. *Nano Energy* **2019**, *57*, 851–871.
- (9) Fan, F. R.; Tian, Z. Q.; Wang, Z. L. Flexible Triboelectric Generator! *Nano Energy* **2012**, *1*, 328–334.
- (10) Chen, J.; Huang, Y.; Zhang, N. N.; Zou, H. Y.; Liu, R. Y.; Tao, C. Y.; Fan, X.; Wang, Z. L. Micro-Cable Structured Textile for Simultaneously Harvesting Solar and Mechanical Energy. *Nat. Energy* **2016**, *1*, 16138.
- (11) Xiong, J. Q.; Cui, P.; Chen, X. L.; Wang, J. X.; Parida, K.; Lin, M. F.; Lee, P. S. Skin-Touch-Actuated Textile-Based Triboelectric Nanogenerator with Black Phosphorus for Durable Biomechanical Energy Harvesting. *Nat. Commun.* **2018**, *9*, 4280.
- (12) Gong, W.; Hou, C. Y.; Zhou, J.; Guo, Y. B.; Zhang, W.; Li, Y. G.; Zhang, Q. H.; Wang, H. Z. Continuous and Scalable Manufacture of Amphibious Energy Yarns and Textiles. *Nat. Commun.* **2019**, *10*, 868.
- (13) Zhao, Z. Z.; Yan, C.; Liu, Z. X.; Fu, X. L.; Peng, L. M.; Hu, Y. F.; Zheng, Z. J. Machine-Washable Textile Triboelectric Nanogenerators for Effective Human Respiratory Monitoring through Loom Weaving of Metallic Yarns. *Adv. Mater.* **2016**, *28*, 10267–10274.
- (14) Dong, K.; Peng, X.; Wang, Z. L. Fiber/Fabric-Based Piezoelectric and Triboelectric Nanogenerators for Flexible/Stretchable and Wearable Electronics and Artificial Intelligence. *Adv. Mater.* **2020**, *32*, 1902549.
- (15) Xiong, J. Q.; Lee, P. S. Progress on Wearable Triboelectric Nanogenerators in Shapes of Fiber, Yarn, and Textile. *Sci. Technol. Adv. Mater.* **2019**, *20*, 837–857.
- (16) Yu, Y.; Qian, X. M. The Effect of Material Performances of Knit Fabric on Clothing Comfort. *Adv. Mater. Res. (Durten-Zurich, Switz.)* **2010**, *156-157*, 717–723.
- (17) Paosangthong, W.; Torah, R.; Beeby, S. Recent Progress on Textile-Based Triboelectric Nanogenerators. *Nano Energy* **2019**, *55*, 401–423.
- (18) Hu, Y. F.; Zheng, Z. J. Progress in Textile-Based Triboelectric Nanogenerators for Smart Fabrics. *Nano Energy* **2019**, *56*, 16–24.
- (19) Yu, W. *Textile Materials*; China Textile Press: Beijing, 2018; pp 414–416.

- (20) Wu, S. H.; Qin, X. H. Uniaxially Aligned Polyacrylonitrile Nanofiber Yarns Prepared by a Novel Modified Electrospinning Method. *Mater. Lett.* **2013**, *106*, 204–207.
- (21) Xiao, H.-M.; Zhang, W.-D.; Na, L.; Huang, G.-W.; Liu, Y.; Fu, S.-Y. Facile Preparation of Highly Conductive, Flexible, and Strong Carbon Nanotube/Polyaniline Composite Films. *J. Polym. Sci., Part A: Polym. Chem.* **2015**, *53*, 1575–1585.
- (22) Wang, Z. L. Triboelectric Nanogenerators as New Energy Technology for Self-Powered Systems and as Active Mechanical and Chemical Sensors. *ACS Nano* **2013**, *7*, 9533–9557.
- (23) Zou, H. Y.; Zhang, Y.; Guo, L. T.; Wang, P. H.; He, X.; Dai, G. Z.; Zheng, H. W.; Chen, C. Y.; Wang, A. C.; Xu, C.; Wang, Z. L. Quantifying the Triboelectric Series. *Nat. Commun.* **2019**, *10*, 1427.
- (24) Peets, P.; Leito, I.; Pelt, J.; Vahur, S. Identification and Classification of Textile Fibres using ATR-FT-IR Spectroscopy with Chemometric Methods. *Spectrochim. Acta, Part A* **2017**, *173*, 175–181.
- (25) Liu, S. R.; Zheng, W.; Yang, B.; Tao, X. M. Triboelectric Charge Density of Porous and Deformable Fabrics Made from Polymer Fibers. *Nano Energy* **2018**, *53*, 383–390.
- (26) Wang, Z. L.; Chen, J.; Lin, L. Progress in Triboelectric Nanogenerators as a New Energy Technology and Self-Powered Sensors. *Energy Environ. Sci.* **2015**, *8*, 2250–2282.
- (27) Wu, R.; Ma, L.; Hou, C.; Meng, Z.; Guo, W.; Yu, W.; Yu, R.; Hu, F.; Liu, X. Y. Silk Composite Electronic Textile Sensor for High Space Precision 2D Combo Temperature-Pressure Sensing. *Small* **2019**, *15*, 1901558.
- (28) Liu, M. M.; Pu, X.; Jiang, C. Y.; Liu, T.; Huang, X.; Chen, L. B.; Du, C. H.; Sun, J. M.; Hu, W. G.; Wang, Z. L. Large-Area All-Textile Pressure Sensors for Monitoring Human Motion and Physiological Signals. *Adv. Mater.* **2017**, *29*, 1703700.